NOx emissions from intermediate-temperature combustion of steel-industry by-product gases

Zoran M. Djurisic*, Eric G. Eddings
Chemical and Fuels Engineering
University of Utah
Salt Lake City, UT 84112-1114

Abstract

A study of NOx emissions from the combustion of coke-oven gas and blast-furnace gas (steel industry by-product gases) was undertaken using detailed kinetic modeling to elucidate the pathways for NOx formation. The study was performed at the intermediate temperatures (1200-1400K) and 1 atm, which represent conditions found in a commercial, ultra-low NOx burner. Simulation results indicated that nitric oxide is formed exclusively in the radical-rich flame zone under these conditions. The traditionally-accepted pathway of Fenimore 'prompt' NO formation, through methylidene and methylene attack on nitrogen molecules, was found to play no role under the conditions of our simulations. In light of this finding, kinetic pathways for NO formation were re-examined. It was found that, according to currently available kinetic parameters, the NO formation is controlled by the H + N_2 reaction. Recently published studies on this reaction, as well as on the rate for the products-set-corrected spin-conserved pathway for the CH + N_2 reaction, agree with our finding that the H + N_2 channel will be the dominant initiation reaction to NO formation from nitrogen molecule. The NOx emissions from our simulations were found to consist almost exclusively of nitric oxide.

Introduction

A traditional steel-making process generates by-product fuels such as blast-furnace gas and coke-oven gas. Blast-furnace gas is a low-heating-value gas with compositions varying widely from plant to plant, but is typically more than 70% inerts (primarily N_2 and CO_2), 20-25% CO, and 5-10% H_2. Coke-oven gas is typically very hydrogen-rich (often 50%), with significant quantities of hydrocarbons and CO, and only small amounts of inert species. These gases are often used as fuels in the steel-making process; however, the NOx formation characteristics have not been widely studied.

Specific objectives

A novel, simple, low-cost burner design was proposed for firing gaseous by-product fuels in industrial boiler [1]. The burner design, based on forced internal recirculation, targets single-digit (vppm) NOx and less than 50 vppm CO emissions without an efficiency penalty. Internal recirculation creates a fuel rich, intermediate temperature flame downstream of the fuel nozzles. As peak flame temperature is kept below 1500 K, and with limited oxygen presence in the primary flame, the thermal (Zeldovich) NOx formation mechanism is suppressed. The focus of this study is in thus identifying the NOx formation and destruction chemical kinetic pathways under these conditions through chemical kinetics simulation.

NOx emissions from six typical fuel blends composed of steel industry by-product gases were examined in this study. The composition of these blends (mole fraction) is provided in Table 1.

Table 1. Composition of fuel blends used in this study

blend	O_2	N_2	H_2	CO	CO_2	CH_4	C_2H_6	H_2O
BFG 0	-	0.470	0.090	0.210	0.230	-	-	-
BFG 1	-	0.876	0.040	0.020	-	0.061	0.003	-
BFG 2	-	0.639	0.044	0.227	0.090	-	-	-
BFG 3	-	0.524	0.046	0.228	0.171	-	-	0.031
COG 0	-	0.070	0.500	0.070	0.010	0.332	0.018	-
COG 1	0.021	0.079	0.328	0.064	-	0.508	-	-
COG 2	-	0.142	0.142	0.071	-	0.612	0.032	-
COG 3	0.002	0.055	0.554	0.056	-	0.311	0.022	-

Since the investigated fuel blends do not contain fuel-bound nitrogen, "prompt NOx" mechanism was expected to be the dominant NOx formation route. The purpose of this study was to verify this hypothesis through detailed kinetics simulation.

Modeling details

A number of published chemical kinetic mechanisms that include NOx chemistry during small-hydrocarbon oxidation were examined for use in this study [2-11]. Comparison of simulation predictions with the experimental data in shock-tube [12-14], isothermal plug-flow reactor [15, 16], well-stirred reactor [17], and

* Corresponding author: djurisic@eng.utah.edu
Associated Web site: http://www.combustion.utah.edu/U-NOx
Proceedings of the Third Joint Meeting of the U.S. Sections of The Combustion Institute

laminar premixed flames [18] identified the mechanisms of Glarborg [7], Dagaut [4], and GRI-Mech 3.0 [11] as the best candidates for this study. Details of these comparisons are published in a separate technical report [19].

All the simulations were performed using Chemkin™ II simulation programs [20-23] and our own post-processing tools for pathway analysis [24].

Results and discussion

In the initial study, the burner was simulated as an isothermal plug-flow reactor at atmospheric pressure, and temperatures ranging from 1200 to 1400 K. We are not aware of any measurements made for oxidation of by-product fuels such as coke oven gas (COG) or blast furnace gas (BFG) in plug flow reactors or well-stirred reactors, and thus we could not evaluate the quality of the kinetic model predictions as applied to these fuels. However, for the purpose of comparing kinetic mechanisms, we simulated with each mechanism the stoichiometric oxidation of BFG0, COG0 and simplified natural gas (95% CH_4 – 5% C_2H_6) in a plug-flow reactor at 1 atm and constant temperature of 1400 K. Conventional understanding of the governing process for NO formation under these conditions is the Fenimore "Prompt" NO mechanism [25], which begins with methylidene attack on molecular nitrogen:

$$CH + N_2 = HCN + N \qquad (1)$$

Quantities of methylidene which should thus initiate the NOx formation, and nitric oxide ultimately produced, agree only qualitatively for blast-furnace gas oxidation when calculated using different kinetic mechanisms. Even the qualitative agreement between methylidene concentrations the different mechanisms is absent for the cases of coke-oven gas and natural gas, with the difference being larger for natural gas. Due to space limitations, in Figure 1 we illustrate these points only for COG0 fuel-blend.

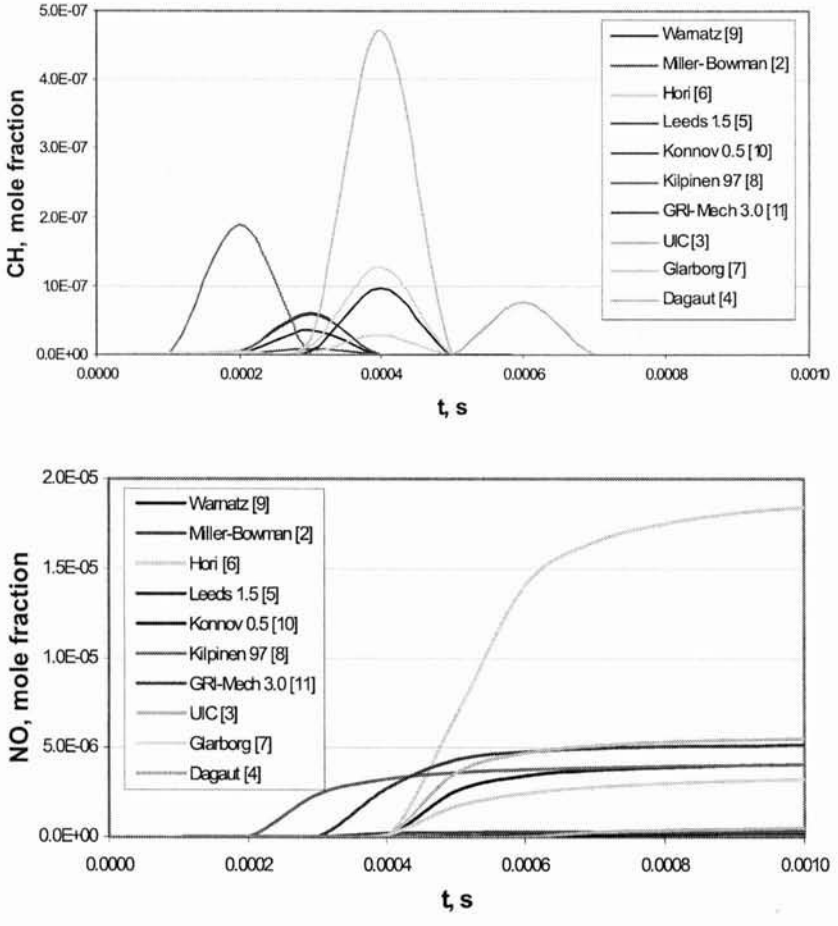

Figure 1. CH and NO concentration profiles for stoichiometric oxidation of COG0 fuel blend in air, predicted by selected kinetic mechanisms. Plug-flow reactor; P = 1 atm; T = 1400 K.

The level of disagreement between different mechanisms, seen in Figure 1, is a reason for caution when interpreting the simulation results in the remainder of this study.

For all the mechanisms considered, simulation results indicate that the major NOx species produced is nitric oxide, with nitrogen dioxide present in concentrations three orders of magnitude lower. None of the mechanisms predicted a net change in NO concentration behind the flame front.

The disagreement in the time of species appearance as predicted by the different mechanisms directly corresponds to the differences in ignition delays predicted by corresponding mechanisms [19]. Comparison of the time of NO appearance and the duration of its concentration increase indicates that the NO production is related to species found in significant quantities only in the flame front. In order to gain insight into the processes governing NO formation for these conditions, pathway analysis was performed. Kinetic paths were explored at the point in the reactor at which the corresponding mechanism predicts the maximum rate of production of NO. Pathways predicted by the different mechanisms are summarized in Figure 2. Major differences between mechanisms are reflected in the portion related to HONO and HCO, indicating underlying differences in formyl chemistry. The pathway presented in the Figure 2 most accurately reflects the predictions by the mechanism of Glarborg [7].

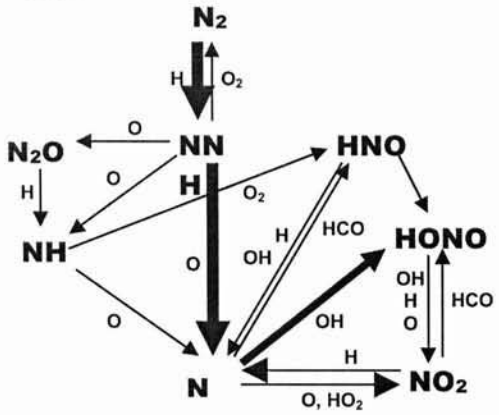

Figure 2. Major NO chemical kinetic pathways at the moment of maximum rate of NO production for coke-oven gas oxidation in a plug flow reactor at 1400 K and 1 atm.

While the absolute reaction rates differ, Figure 2 represents also blast-furnace gas and simplified natural gas oxidation under the same conditions.

This pathway diagram indicates no influence of hydrocarbon fragments, methylidene in particular, to NO emissions other than second-order effects through the H-O-OH radical pool. There is large uncertainty in kinetic data for reaction (1), with the reaction rate coefficient spanning more than five orders of magnitude between different kinetic mechanisms. Difficulties in preparing methylidene radicals have prevented direct measurement of the reaction rate. Existing experimental values have been obtained indirectly, or through modeling, by adjusting the reaction rate to fit the experimental CH or NO profiles in a combustion device.

A number of experimental and theoretical studies have focused on reaction (1), even though some researchers had recognized a fundamental problem with this reaction arising from the fact that the angular momentum would not be conserved during the doublet/quartet surface crossing. Recently Moskaleva and Lin [26] resolved the problem finding the physically acceptable reaction path that indicates the overall reaction:

$$CH + N_2 = H + NCN \quad (2)$$

The proposed temperature-dependent rate coefficient for this reaction is of the order of magnitude of the lowest of the rate coefficients for CH + N_2 found in tested mechanisms (i.e. mechanism of Glarborg). This new lower rate coefficient (not used in any of the detailed mechanisms yet) further suggests no direct involvement of methylidene in NO formation.

On the other hand, several recent studies [27-30] have indicated that there might be another reaction channel involving attack of N_2 molecule:

$$H + N_2 = N + NH \quad (3)$$

or

$$H + N_2 = NNH \quad (4)$$

This work is, however, the first study to indicate hydrogen atom attack as the dominant initiation step. As the reaction pathways in Figure 2 suggest, reaction (4) appears to be the only path leading to N≡N bond scission. This result is not surprising if one considers that the peak concentration of hydrogen atom is between three to eight orders of magnitude higher than that of methylidene, even though their appearance in hydrocarbon flames occurs at the same time. This high hydrogen atom concentration, coupled with a significantly larger rate coefficient, ensures that the NNH channel (4) becomes the dominant path to NO formation at intermediate temperatures and atmospheric pressure, independent of the presence of hydrocarbon fragments.

In collaboration with Truong and Huynh [31] we re-examined the rate coefficient for the reaction (4). In preliminary *ab-initio* study, geometries, energies and vibrational frequencies of stable species and the transition state were determined at the quadratic configuration interaction with all single and double excitations (QCISD) level of theory using the augmented correlation-consistent triple-zeta plus polarization (aug-cc-pVTZ) basis set. The forward barrier was found to be 61.5 kJ/mol, which is only about 2.1 kJ/mol lower than previously reported

value [27]. However, the reverse barrier of 26.0 kJ/mol is much lower than the value of 47.3 kJ/mol determined previously [27]. This difference would have an effect on the lifetime of the NNH radical. We have calculated temperature-dependent rate coefficient for the reaction (4) using the conventional transition state theory augmented by one-dimensional Eckart tunneling corrections. In the high-pressure limit, we obtained

$$k_{4,f} = 1.082 \cdot 10^{13} \theta^{0.838} e^{-\frac{6592}{T}}, \quad \frac{\text{cm}^3}{\text{mol} \cdot \text{s}}$$

$$k_{4,r} = 4.306 \cdot 10^{12} \theta^{0.846} e^{-\frac{2849}{T}}, \quad \frac{1}{\text{s}}$$

for forward and reverse reactions, respectively, and θ is the nondimensional temperature, defined as T/298 K.

NOx emissions prediction for COG and BFG blends

BLAST-FURNACE GAS MIXTURES

Using the mechanism of Glarborg [7], which was the mechanism that provided the best representation of the experimental data, simulations of oxidation in a plug-flow reactor for given BFG and COG formulations were performed. In all cases presented in the following discussion, the qualitative properties of the predictions were verified by use of additional simulations based on the GRI-Mech 3.0 and Dagaut mechanisms.

NO emissions from the oxidation of four BFG formulations in a plug-flow reactor are presented in Figure 3. Except for BFG 1, NO emissions follow the same trend regardless of differences in composition. The difference in NO emission levels between BFG 0, BFG 2, and BFG 3, is related directly to the difference in the nitrogen molecule concentration in the unreacted mixture. In all 3 cases, the NO emissions levels span roughly a factor of two, with the peak on the fuel-lean side (ϕ= 0.8), at 5 – 7 ppm (not shown). For comparison, the two other mechanisms, used as a control, predicted NO levels a factor of 5 and 10 lower, respectively. While we recommend the mechanism of Glarborg for use under these conditions, the absolute levels of NO predicted should serve only as a rough estimate, until measurements under these conditions provide firmer support.

For all four mixtures investigated, reaction kinetic pathway analysis showed that the NO formation closely follows the paths presented in Figure 2, with N_2 + H being the dominant initiation channel.

In contrast to the three other BFG formulations, NO emission patterns during BFG 1 oxidation differed significantly, and additional simulations were performed in order to elucidate the difference. Through the course of several steps, the original BFG 1 formulation was gradually simplified to identify the impacts of key species. Simulation results, after substitution of CO_2 and CO by either argon or nitrogen, demonstrated that the difference in the emission patterns lies in the hydrogen-hydrocarbon interaction, which is not present in the other 3 mixtures.

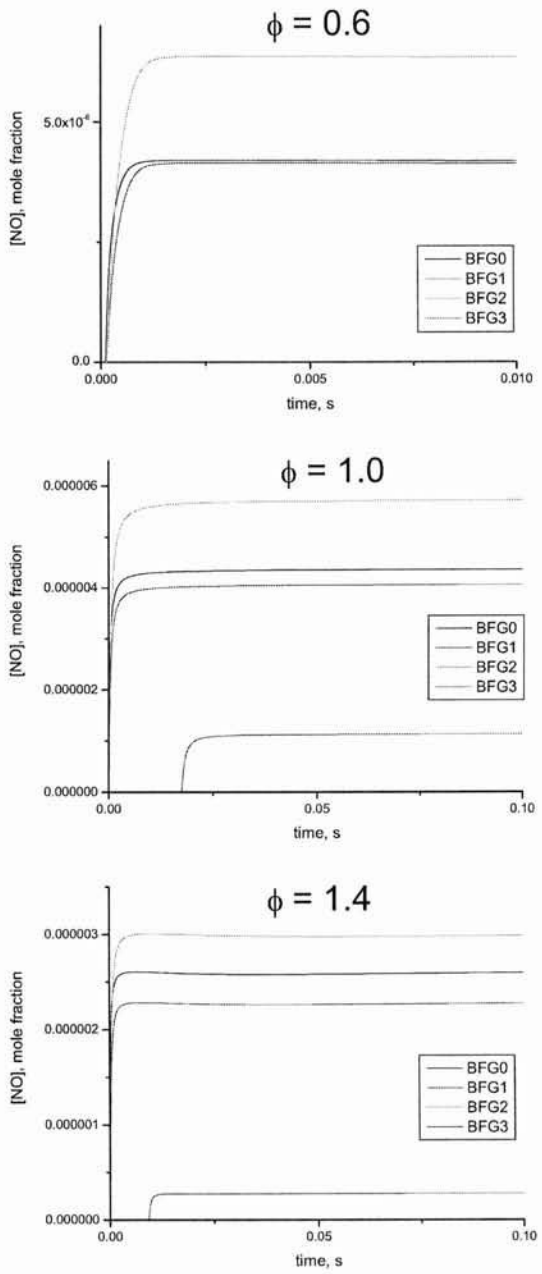

Figure 3. NO concentration profiles in a plug-flow reactor during BFG oxidation at 1200 K and 1 atm.

As can be seen in Figure 4, NO production closely follows the availability of hydrogen atom. A comparison between the two cases (BFG 0 and BFG 1) presented in Figure 4 indicated that the hydrogen atom production

becomes a two-stage process in the presence of hydrocarbons.

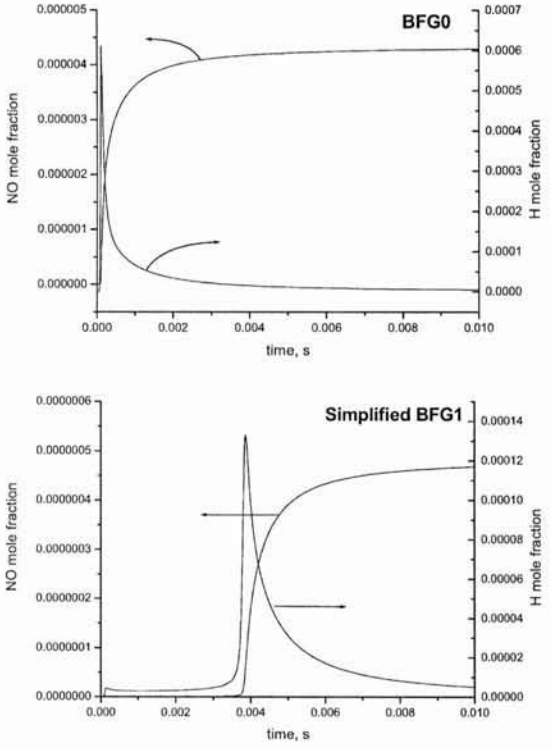

Figure 4. H and NO concentration profiles during BFG oxidation in a plug flow reactor at 1200 K and 1 atm. Upper diagram: BFG 0; lower diagram: H_2/CH_4. Note magnitude difference in y-axis scales.

As seen with the case of a H_2/CH_4 mixture used as a fuel (which represents a simplified BFG1 blend), the first step in H atom production appears at the same time as the hydrogen atom peak for BFG0 (top diagram in Figure 4), at 100 μs from the reactor inlet. In the simplified BFG1 case (bottom diagram), however, the net rate of the production of the hydrogen atom temporarily drops to zero, and the appearance of the main peak is significantly postponed. Reaction kinetic pathway analysis indicates that the reason for the difference between the two cases lies in the hydrogen-hydrocarbon interaction. Namely, the first stage in hydrogen atom production for simplified BFG1 case does correspond to molecular hydrogen ignition, and this governing process is identical to the ignition process in BFG0 case. However, as the hydrogen atom concentration increases, hydrocarbons present in the BFG1 case become an effective sink for hydrogen atoms through the reactions:

$$CH_4 + H \rightarrow CH_3 + H_2 \quad (5)$$

$$C_2H_6 + H \rightarrow C_2H_5 + H_2 \quad (6)$$

$$C_2H_5 + H \rightarrow C_2H_4 + H_2 \quad (7)$$

While reaction (5) has a significantly higher activation energy than reactions (6) and (7), the larger CH_4 concentration makes reaction (5) still the dominant hydrogen atom sink for the duration of CH_4 availability. Besides the higher peak H concentration in the BFG 0 case, integration through the reactor of the hydrogen atom concentration profiles for the two cases reveals that the total quantity of hydrogen atom available is also twice as large for the BFG 0 case.

Since the presence of the hydrocarbons dramatically affected the NO emissions, additional simulations were performed to gain insight into the influence of the hydrogen-to-hydrocarbons ratio. These simulations were performed on stoichiometric H_2/CH_4/air mixtures at 1200 K, with the H_2:CH_4 ratio varying from 0 to ∞. The variation of the ignition delay and the NO emissions are presented in Figure 5.

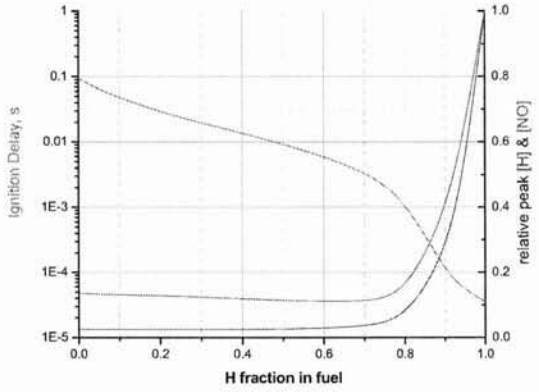

Figure 5. Ignition delay and NO emissions for the stoichiometric oxidation of a methane/hydrogen mixture in a plug flow reactor at 1200 K and 1 atm. The fuel composition varies from pure methane to pure hydrogen

The simulation results suggest that the presence of small quantities of hydrocarbons in an unreacted H_2/air mixtures can dramatically decrease NO emissions by scavenging free hydrogen atoms. The presence of hydrocarbons at a level of 20% of hydrogen (on a molar basis) was sufficient to achieve a 10-fold reduction in the exhaust NO levels.

COKE-OVEN GAS MIXTURES

NOx emissions from coke-oven gas oxidation in a plug-flow reactor were performed under the same conditions as for the previously presented blast-furnace gas. The simulation results are shown in Figure 6. Analysis of the NO emissions from the different coke-oven gas formulations indicate that the NO emissions levels are similar in magnitude for all four compositions. The NO levels are also a strong, asymmetric function of the reactant stoichiometry, with peak emissions at

stoichiometric conditions and a sharp drop on the fuel–lean side. The differences in COG composition for the four cases did not influence NO emissions levels. However, the appearance of hydrogen atom, and consequently the onset of NO production, was strongly influenced by the reactants composition. The mechanism for ignition delay appears to be the same as for BFG1, since the longer ignition delay occurs for COG1 and COG2, for which hydrocarbons dominate (on a molar basis) over hydrogen. For the other two cases (COG0 and COG3) the mole fraction of hydrogen is larger than for hydrocarbons, decreasing the time to ignition, but the H_2:hydrocarbon ratio is still too low (around 60:40 in both cases) to allow a significant increase in hydrogen atom concentration and subsequent increase in NO. Results indicate a net NO sink under fuel lean conditions for all four mixtures.

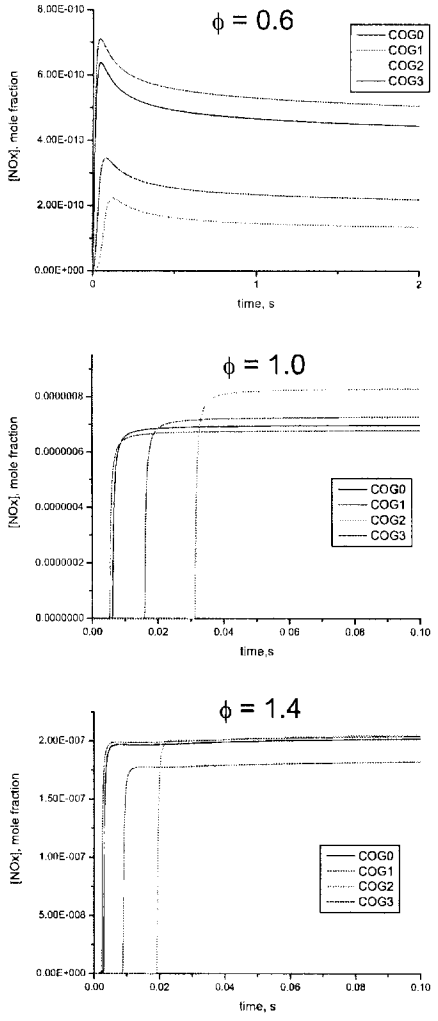

Figure 6. NO concentration profiles in a plug-flow reactor during COG oxidation at 1200 K and 1 atm.

Employing again reaction kinetic pathway analysis, we concluded that the net decrease of NO in later stages of combustion under fuel lean conditions is due to recycling of NO to N_2, which is initiated by the conversion to HCN through the reaction:

$$NO + HCCO \rightarrow HCN + CO_2 \qquad (8)$$

Although the ketyl radical appears at higher peak concentrations in stoichiometric and fuel-rich conditions, its existence for the fuel-lean case in quantities that are not negligible extends much further downstream, to the area where NO production channels have become insignificant.

Conclusions

In the present study, investigations were made on NO emissions from low-BTU by-product fuels available in the steel industry. The analysis focused on NO emissions under conditions typical of an ultra-low NOx gas burner, where internal recirculation dilutes reactants and keeps the flame temperature in the range of 1200 – 1400 K.

Twelve detailed kinetic mechanisms were tested against experimental data in order to identify the best available detailed mechanism to describe NOx chemistry under FIR operating conditions. While none of the mechanisms describes all of the data to a satisfactory level, the Glarborg 1998, GRI-Mech 3.0 and Dagaut 2000 mechanisms were identified as being sufficiently good for providing qualitative, and to a lesser confidence level, quantitative description of the NOx chemistry.

Under the intermediate-temperature burner conditions, thermal NO reaction channels are insignificant, and the NO production occurs only in the flame zone, which is rich in free radicals. Contrary to a long-held belief that such "prompt" NOx formation is initiated by N≡N bond scission due to methylidene attack, we suggest that the recently-proposed hydrogen atom attack is solely responsible for subsequent N≡N bond scission under the investigated conditions. Furthermore, no case was found in which the direct involvement of hydrocarbon fragments would play a role in N≡N bond scission. In all the cases analyzed in this study, NOx emissions were composed of over 99% nitric oxide (NO).

Interaction between hydrogen and hydrocarbons was recognized as being extremely important in controlling NO emission levels through the hydrogen atom removal. The presence of at least 20% hydrocarbons, relative to the hydrogen content, resulted in dramatically lower NO emissions as compared to a fuel in which no hydrocarbons were present. All other components present in both blast-furnace gas and coke-oven gas were found to have negligible influence on NOx emissions under the conditions investigated.

Acknowledgements

The authors gratefully acknowledge funding for this work provided by the Gas Technology Institute through a grant with the U.S. Department of Energy. Additional funding was provided by Reaction Engineering International and the University of Utah Research Fund.

References

1. http://www.oit.doe.gov/combustion/ /rd_portfolio_forced.shtml
2. Miller J. A., Bowman C. T., *Prog. Energy Combust. Sci.*, 15, 287-338, 1989.
3. Mosiewicz P., Porshnev P., Nester S., Kennedy L. A., Fridman A., Rabovitser J., Cygan D., *Combust. Sci. and Tech.*, 160, 1-21, 2000.
4. Dagaut P., Luche J., and Cathonnet M., *Energy & Fuels*, 14, 712-719, (2000)
5. Hughes K. J., Turanyi T., and Pilling M. J., http://www.chem.leeds.ac.uk/Combustion/Combustion.html, Mar 2001.
6. Hori M., Matsunaga N., Marinov N., Pitz W., and Westbrook C., 27th symposium (International) on Combustion/The Combustion Institute, 1998/pp. 389–396
7. Glarborg P., Alzueta, Dam-Johansen K., and Miller J. A., *Combust. Flame* 115:1-27, 1998.
8. Kilpinen, P., Åbo Akademi University - PCG, Detailed Kinetic Scheme "Kilpinen 97", http://www.abo.fi/fak/ktf/cmc.
9. Klaus P. and Warnatz J., International Workshop on Measurement and Computation of Turbulent Nonpremixed Flames, July 1997.
10. Konnov, A. A. Detailed reaction mechanism for small hydrocarbons combustion. Release 0.5 http://homepages.vub.ac.be/~akonnov/, 2000.
11. Smith G. P., Golden D. M., Frenklach M., Moriarty N. W., Eiteneer B., Goldenberg M., Bowman C. T., Hanson R. K., Song S., Gardiner W. C. Jr., Lissianski V. V., and Qin Z., http://www.me.berkeley.edu/gri_mech
12. Spadaccini L. J. and Colket M. B., *Prog. Energy Combust. Sci.*, 20, 431, 1994.
13. Yang, H., Qin, Z., Lissianski, V. V., and Gardiner, W. C., *Israel Journal of Chemistry*, 36(3), 305, 1996.
14. Westbrook C. and Pitz W. J., *Combust. Sci. Technol.*, 33, 315-319, 1983.
15. Miller, J.A. and Glarborg, P. Springer Series in Chemical Physics; Springer-Verlag: Berlin, Germany, 1996.
16. Alzueta M. U., Glarborg P., and Dam-Johansen K., *Combust. Flame*, 109 (1/2), 25-36, 1997.
17. Lecomte F., Dagaut P., Chevailler S., and Cathonnet M., *Combust. Sci. Tech.*, 150 , 181-203, 2000.
18. Bhargava A. and Westmoreland P R., *Combust. Flame*, 113, 333-347, 1998.
19. Djurisic Z. M. and Eddings G. E., "Selection of detailed chemical kinetic model for the simulation of nitrogen oxide chemistry during natural gas combustion at Intermediate temperatures", final report for the Gas Technology Institute, subcontract No. PF8680, November 2002.
20. Kee, R. J., Rupley, F. M., and Miller, J. A. (1989) "CHEMKIN-II: A Fortran chemical kinetics package for the analysis of gas-phase chemical kinetics", Sandia National Laboratories Report SAND89-8009
21. Lutz, A. E., Kee, R. J., and Miller J. A. (1987) "SENKIN: A Fortran program for predicting homogeneous gas phase chemical kinetics with sensitivity analysis", Sandia National Laboratories Report SAND87-8248
22. Glarborg, P., Kee, R. J., Grcar, J. F., and Miller, J. A. (1986) "PSR: A Fortran program for modeling well-stirred reactors", Sandia National Laboratories Report SAND86-8209
23. Kee, R. J., Grcar, J. F., Smooke, M. D., and Miller, J. A. (1985) "A Fortran program for modeling steady laminar one-dimensional premixed flames", Sandia National Laboratories Report SAND85-8240.
24. Djurisic Z. M., U-NOx online computational framework and data-center, http://www.combustion.utah.edu/U-NOx
25. Fenimore C. P., 13th Symposium (International) on Combustion, The Combustion Institute, Pittsburgh, 373-380, 1970.
26. Moskaleva L. V. and Lin M. C., *28th Symposium (International) on Combustion*, Edinburgh, Scotland, 2393-2401, 2000.
27. Bozzelli, J. W. and Dean A. M., *Int. J, Chem. Kin.*, **27**, 1097-1109, 1995.
28. Hayhurst A. N. and Hutchinson E. M., *Combust. Flame*, 114, 274-279, 1998.
29. Konnov A. A., Colson G., and de Ruyck J., *Combust. Flame*, 121, 548-550, 2000.
30. Tomeczek J. and Gradon B., *6th International Conference on technologies and combustion for a clean environment*, Proceedings, 513-520, 2001.
31. Truong T., Huynh, L. K., private communication, 2002.